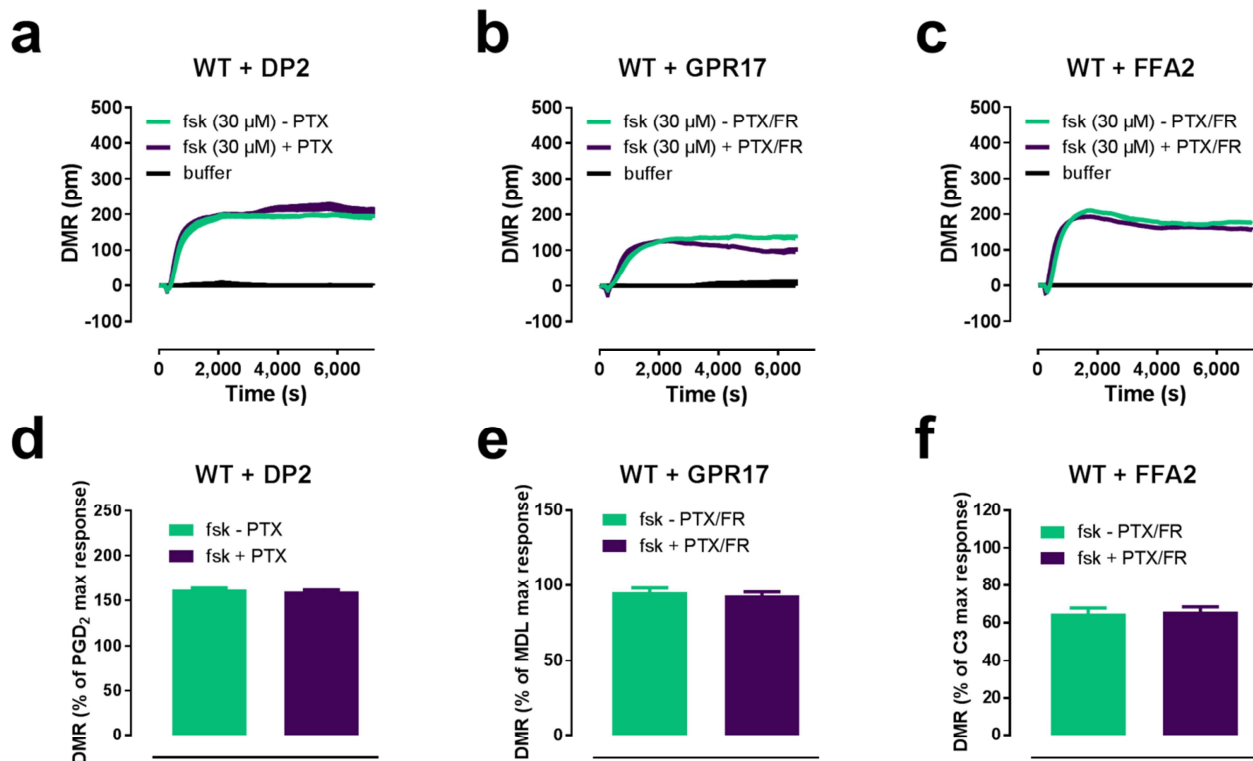
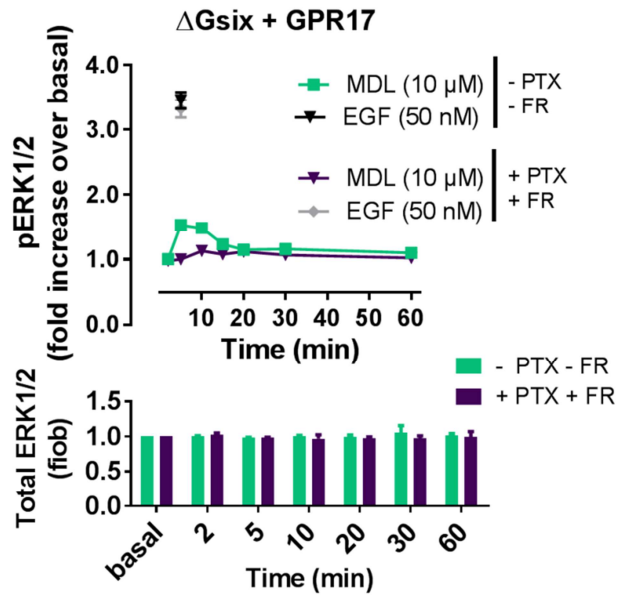


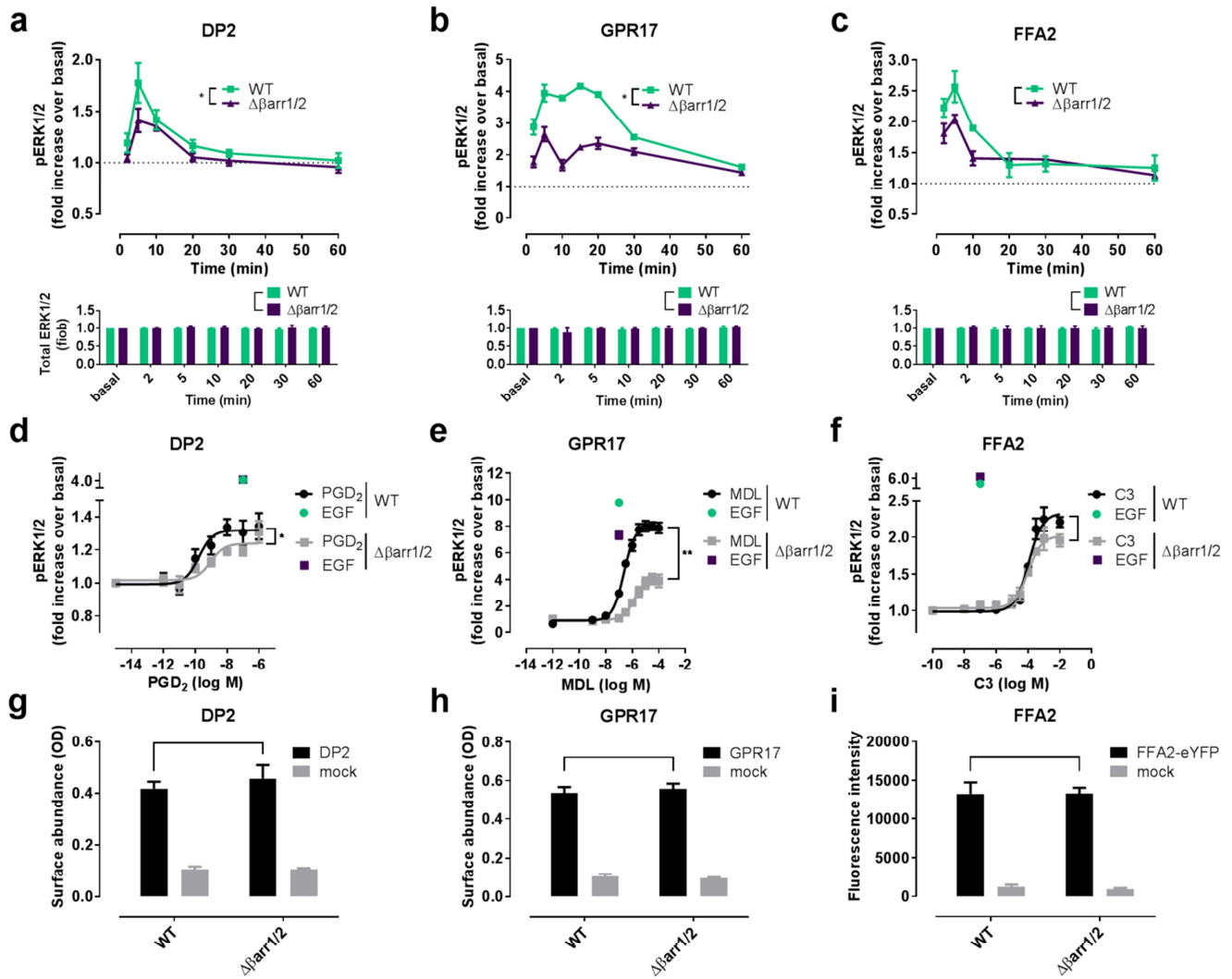
**Supplementary Figure 1. Biochemical and functional characterization of  $\Delta Gsix$  cells.** (a-e) Western blots of wild-type,  $\Delta Gq/11/12/13$  and  $\Delta Gsix$  HEK293 cell lysates probed with antibodies against  $G\alpha_{q/11/14}$  (a),  $G\alpha_{12}$  (b),  $G\alpha_{13}$  (c),  $G\alpha_{s/olf}$  (d) and  $G\alpha_i$  (e). Uncropped blots are available in Supplementary Fig. 17. (f) cAMP levels after stimulation of vasopressin V2 receptor (V2R) or mock transfected wild-type and  $\Delta Gsix$  cells with the indicated compounds or vehicle for 10 minutes. (g,h) DMR traces of  $PGD_2$ -stimulated DP2 receptor in  $\Delta Gsix$  HEK293 cells in absence (g) and presence (h) of PTX. (i) Concentration-response-curve of peak value data from (g) and (h). (j,k) Real-time whole cell response of  $\Delta Gsix$  (j) and wild-type (k) HEK293 cells upon stimulation with 30 nM epidermal growth factor (EGF). (a-e) Representative blots of 2 independent experiments. (f,i) Data are mean  $\pm$  SEM of 3 independent experiments. (g,h,j,k) Shown are representative traces (mean + SEM) of 3 independent experiments, each performed in triplicate.



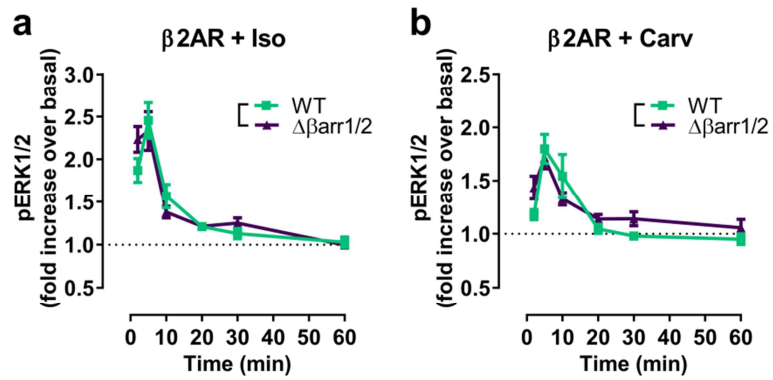
**Supplementary Figure 2. Forskolin-mediated DMR in the absence and presence of signal transduction inhibitors PTX and FR.** (a-c) Forskolin (fsk)-induced DMR traces of DP2 (a), GPR17 (b), or FFA2 (c) wild-type HEK293 cells in absence and presence of G protein inhibitors. (d-f) Quantification of fsk-mediated DMR responses from conditions in (a-c). (a-c) Shown are representative traces (mean + SEM) of 3 independent experiments, performed in triplicate wells for each condition. (d-f) AUC of DMR traces over the entire measurement time was analyzed and presented as mean values + SEM of 3 independent experiments (3 technical replicates).



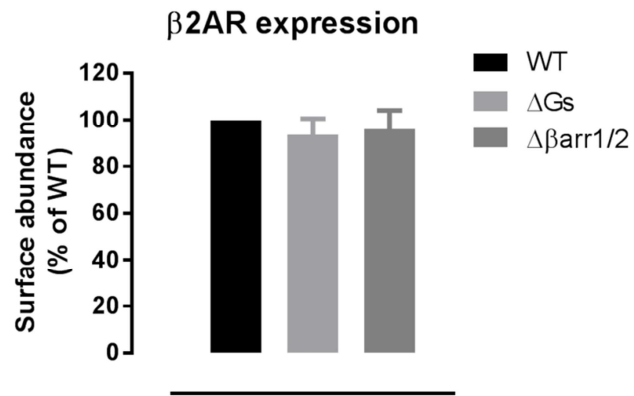
**Supplementary Figure 3. G protein-dependence of ERK1/2 phosphorylation for the GPR17 receptor.** 10  $\mu$ M MDL-induced kinetic pERK1/2 and total ERK profile of GPR17 in  $\Delta$ Gsix cells (+/- PTX/FR). Data are mean  $\pm$  SEM of 3 independent experiments, each measured in triplicates. Fio, fold increase over basal.



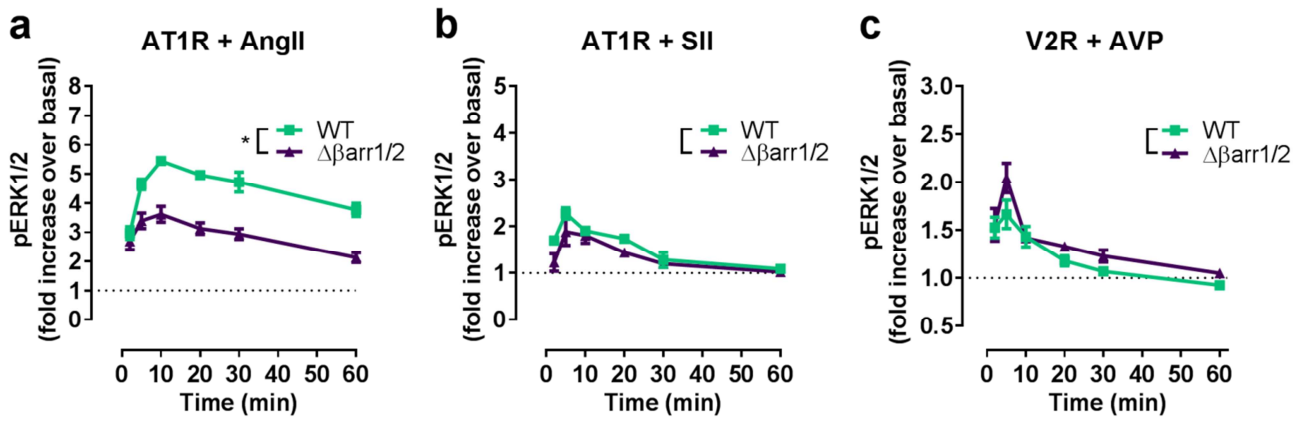
**Supplementary Figure 4. Comparative analysis of ERK1/2 phosphorylation and cell surface abundance of DP2, GPR17 and FFA2 in parental HEK293 and  $\Delta\betaarr1/2$  cells.** (a-c) pERK1/2 and total ERK1/2 kinetic profile of DP2 (a), GPR17 (b), and FFA2 (c) in wild-type and  $\Delta\betaarr1/2$  cells stimulated with 1  $\mu\text{M}$  PGD<sub>2</sub> (a), 10  $\mu\text{M}$  MDL (b), and 100  $\mu\text{M}$  C3 (c). (d-f) Concentration-effect-curves of pERK1/2 levels after 5 minutes stimulation of WT and  $\Delta\betaarr1/2$  cells expressing DP2 (d, pEC<sub>50</sub>: 9.78 $\pm$ 0.32 (WT); 9.0 $\pm$ 0.35 ( $\Delta\betaarr1/2$ )), GPR17 (e, pEC<sub>50</sub>: 6.64 $\pm$ 0.7 (WT); 5.86 $\pm$ 0.14 ( $\Delta\betaarr1/2$ )) or FFA2 (f, pEC<sub>50</sub>: 4.0 $\pm$ 0.1 (WT); 4.0 $\pm$ 0.12 ( $\Delta\betaarr1/2$ )) with their cognate agonist. (g-i) Quantification of receptor expression in wild-type and  $\Delta\betaarr1/2$  cells of DP2 (g), GPR17 (h), and FFA2eYFP (i). Data are mean  $\pm$  SEM of 3 independent experiments (3 technical replicates). For statistical analysis, two-sample paired Wilcoxon test was applied to paired points at different times (a-c) or at different concentrations (d-f) and two-tailed paired t-test (g-i) were performed. \*, P<0.05; \*\*, P<0.01; not significant where no asterisk. Fiob, fold increase over basal.



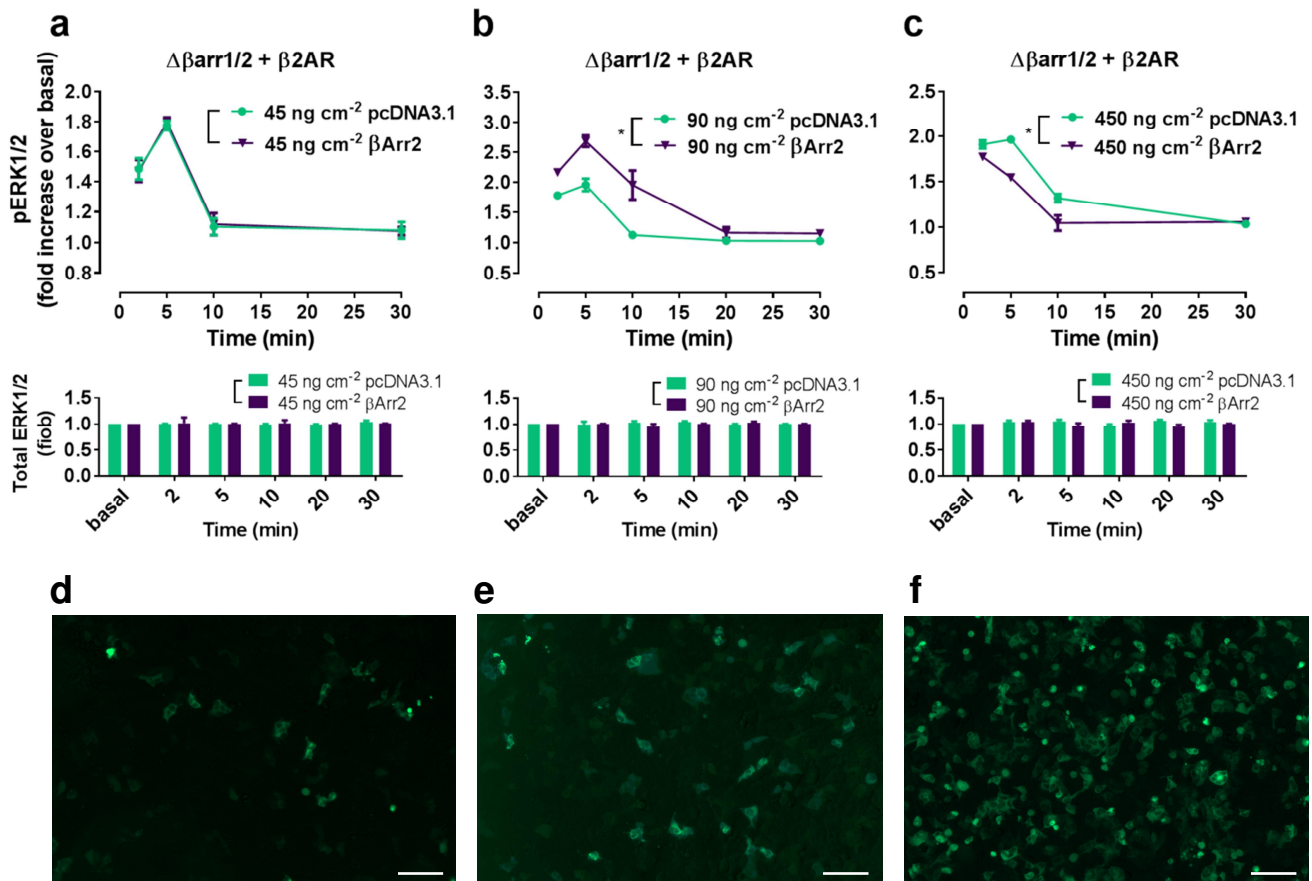
**Supplementary Figure 5. Comparative analysis of ERK1/2 phosphorylation for ligand-stimulated  $\beta 2AR$  in parental HEK293 and  $\Delta\beta arr1/2$  cells. (a,b) pERK1/2 kinetic profiles of  $\beta 2AR$  in wild-type parental and  $\Delta\beta arr1/2$  HEK293 cells stimulated with 10  $\mu M$  isoproterenol (Iso) (a) and 10  $\mu M$  carvedilol (Carv) (b). Data are mean  $\pm$  SEM of 4 independent experiments (3 technical replicates each). For statistical analysis, two-sample paired Wilcoxon test was applied to paired points at different times; not significant where no asterisk.**



**Supplementary Figure 6. Cell surface abundance of β2-adrenergic receptor (β2AR) in different HEK293 cell lines.** Surface ELISA detecting N-terminally HA-tagged β2AR in wild-type, ΔGs and Δβarr1/2 HEK293 cells. Data are mean + SEM of 3 independent experiments, performed in triplicate.

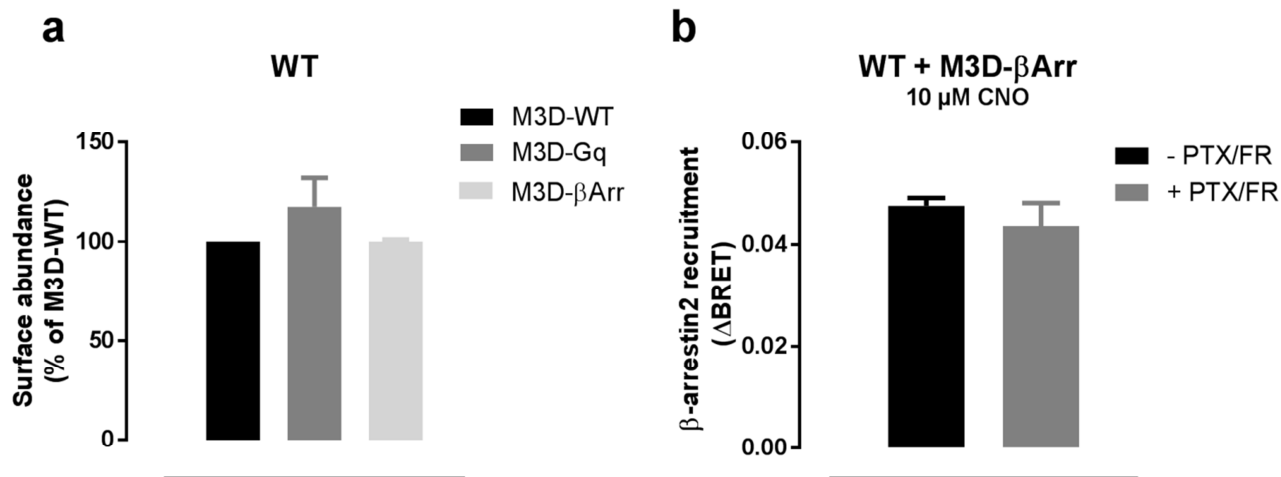


**Supplementary Figure 7. Comparative analysis of ERK1/2 phosphorylation for ligand-stimulated AT1R and V2R in parental HEK293 and  $\Delta\betaarr1/2$  cells.** (a-c) pERK1/2 kinetic profiles of AT1R (a,b) and V2R (c) in wild-type parental and  $\Delta\betaarr1/2$  HEK293 cells stimulated with 100 nM angiotensin II (AngII) (a), 30  $\mu$ M [Sar<sup>1</sup>, Ile<sup>4</sup>, Ile<sup>8</sup>]AngII (SII) (b), and 1  $\mu$ M arginine-vasopressin (AVP) (c). Data are mean  $\pm$  SEM of 4 (AT1R in WT), 5 (AT1R in  $\Delta\betaarr1/2$ ), and 3 (V2R) independent experiments (3 technical replicates each). For statistical analysis, two-sample paired Wilcoxon test was applied to paired points at different times. \*, P<0.05; not significant where no asterisk.

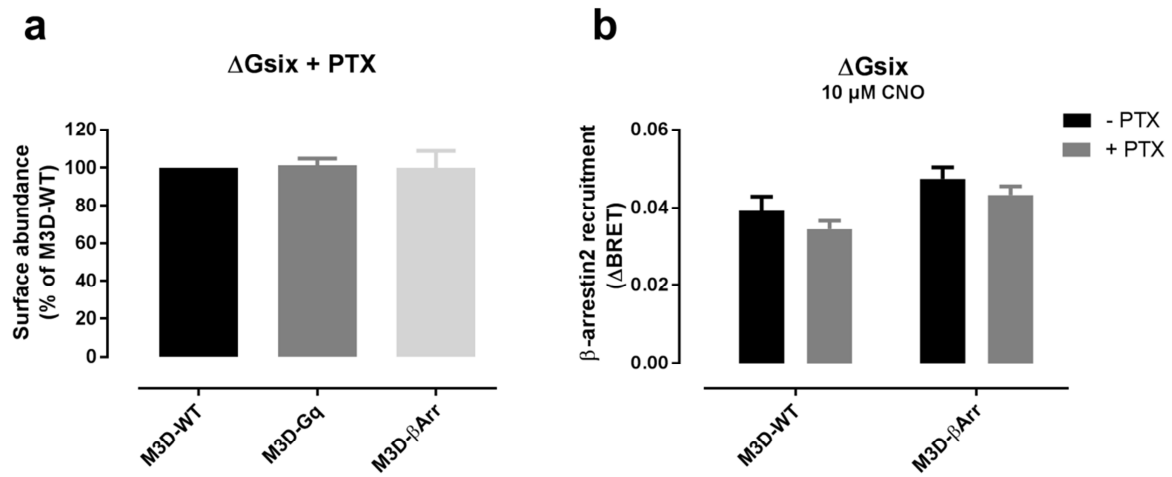


**Supplementary Figure 8. Impact of increasing  $\beta$ -arrestin2 amounts on  $\beta\text{2AR}$ -mediated pERK1/2 kinetics.** (a-c) Kinetic ERK1/2 phosphorylation and total ERK profile of 10  $\mu\text{M}$  Isoproterenol-stimulated  $\Delta\beta\text{arr1/2}$  cells stably transfected with  $\beta\text{2AR}$  and transiently transfected with either empty vector (pcDNA3.1) or a range of  $\beta$ -arrestin2-GFP ( $\beta\text{Arr2}$ ) amounts. (d-f) Fluorescence imaging of  $\beta$ -arrestin2 transfected cells for each condition in a-c. (a-c) Data are mean  $\pm$  SEM of 4 independent experiments (3 technical replicates). For statistical analysis, two-sample paired Wilcoxon test was applied to paired points at different times. \*,  $P < 0.05$ ; not significant where no asterisk. (d-f) Representative images of 4 independent experiments. Scale bar is 100  $\mu\text{m}$ .

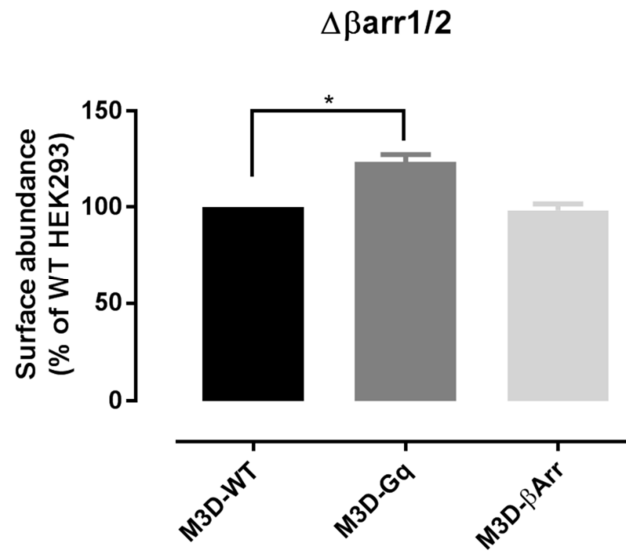




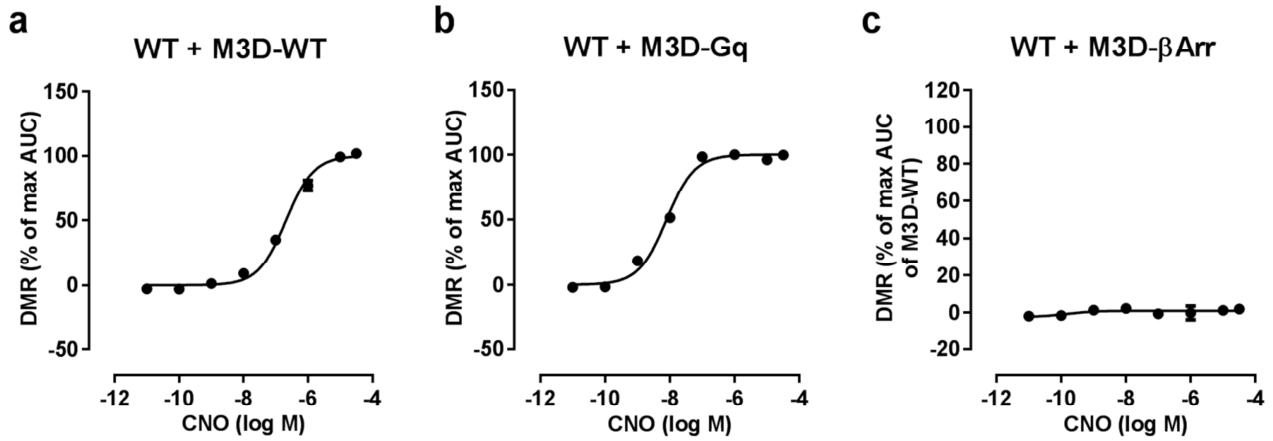
**Supplementary Figure 9. Cell surface abundance and functionality of M3D-βArr in wild-type HEK293 cells.** (a) Surface amounts of N-terminally HA-tagged DREADD constructs (M3D-WT, M3D-Gq, M3D-βArr) in wild-type (WT) HEK293 cells. (b) CNO-induced β-arrestin2 recruitment of the M3D-βArr receptor in absence (black) and presence (grey) of G protein inhibitors (PTX/FR). Data are mean + SEM of 3 independent experiments, each measured in triplicates.



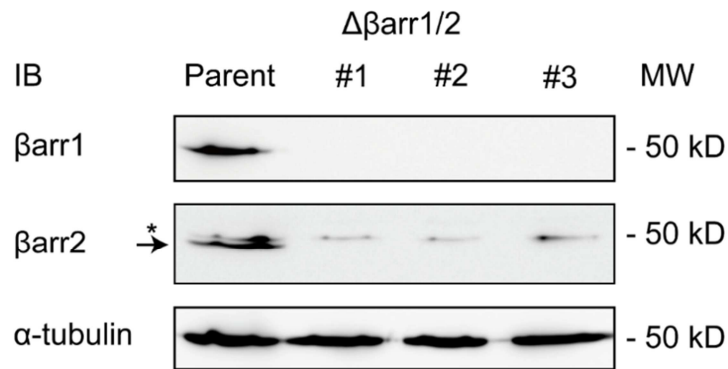
**Supplementary Figure 10. Cell surface DREADD abundance and  $\beta$ -arrestin2 recruitment in the absence of G proteins.** (a), Surface ELISA of N-terminally HA-tagged DREADD constructs (M3D-WT, M3D-Gq, M3D- $\beta$ Arr) in HEK293 cells collectively lacking G proteins ( $\Delta$ Gsix + PTX). (b)  $\beta$ -arrestin2 recruitment by M3D-WT and M3D- $\beta$ Arr receptors upon CNO stimulation in cells either partially ( $\Delta$ Gsix, black) or collectively ( $\Delta$ Gsix + PTX, grey) depleted of G proteins. Data are mean + SEM of 3 independent experiments (3 technical replicates).



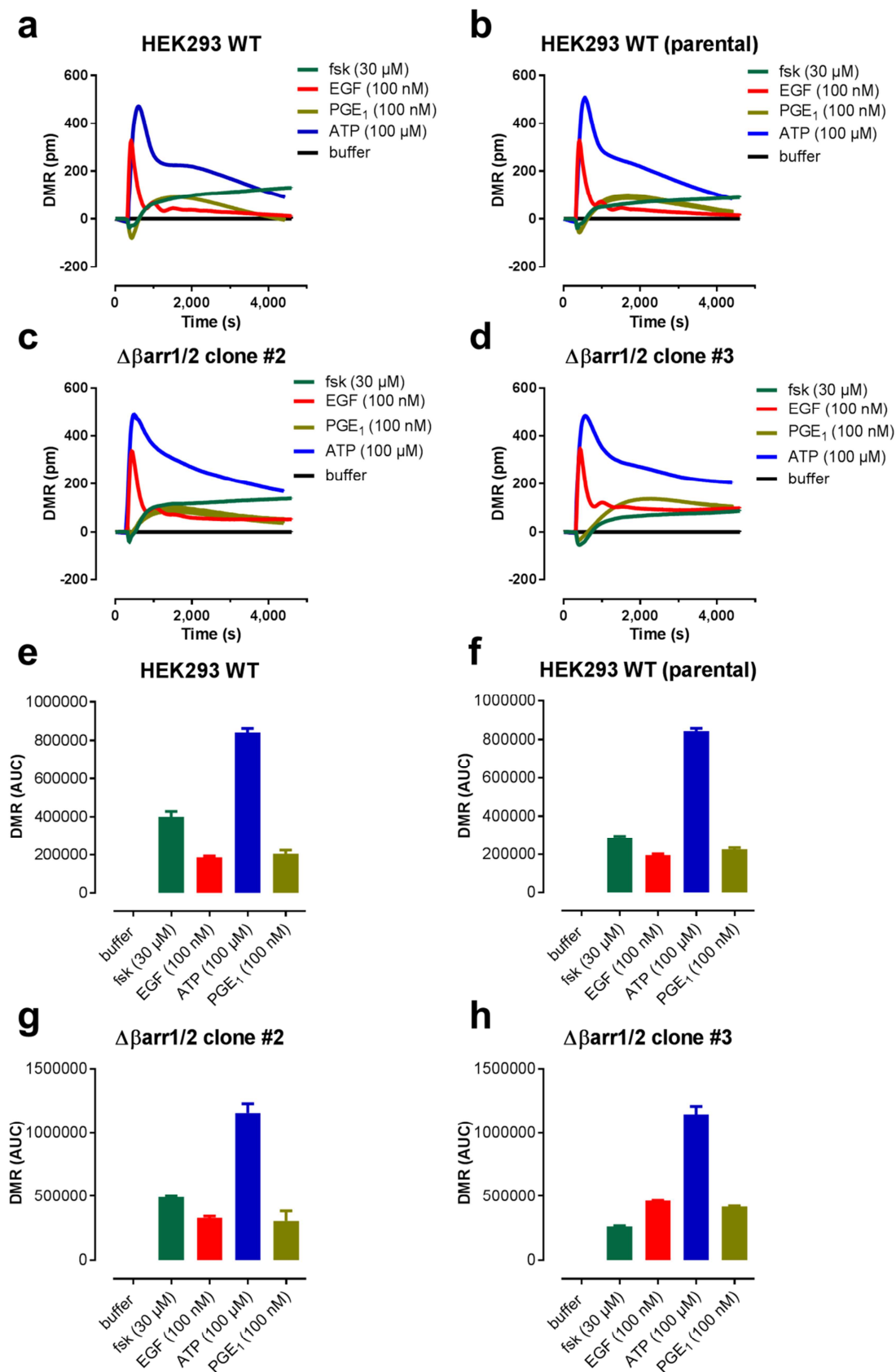
**Supplementary Figure 11. DREADD cell surface abundance in  $\Delta\betaarr1/2$  cells.** Surface ELISA of N-terminally HA-tagged DREADD constructs (M3D-WT, M3D-Gq, M3D- $\beta$ Arr) in  $\Delta\betaarr1/2$  cells, normalized to surface abundance of receptors in WT HEK293 cells (100%). Data are mean + SEM of 3 independent experiments, performed in triplicate. For statistical analysis, one sample t-test was performed. \*,  $P < 0.05$ .



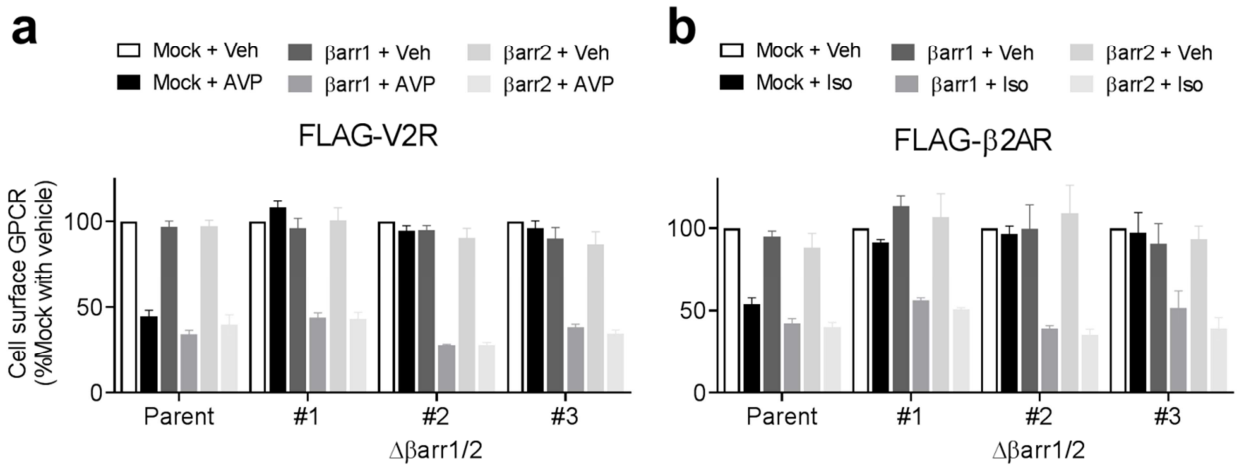
**Supplementary Figure 12. Concentration-effect curves of DMR recordings for CNO-activated DREADDs in HEK293 cells.** Quantification of CNO-induced DMR response in wild-type HEK293 cells expressing the M3D-WT (pEC<sub>50</sub>: 6.68) (a), the M3D-Gq (pEC<sub>50</sub>: 8.12) (b), or the M3D-βArr (c) receptor. AUC of DMR traces over the entire measurement time was analyzed and presented as mean values ± SEM of 3 independent experiments (3 technical replicates).



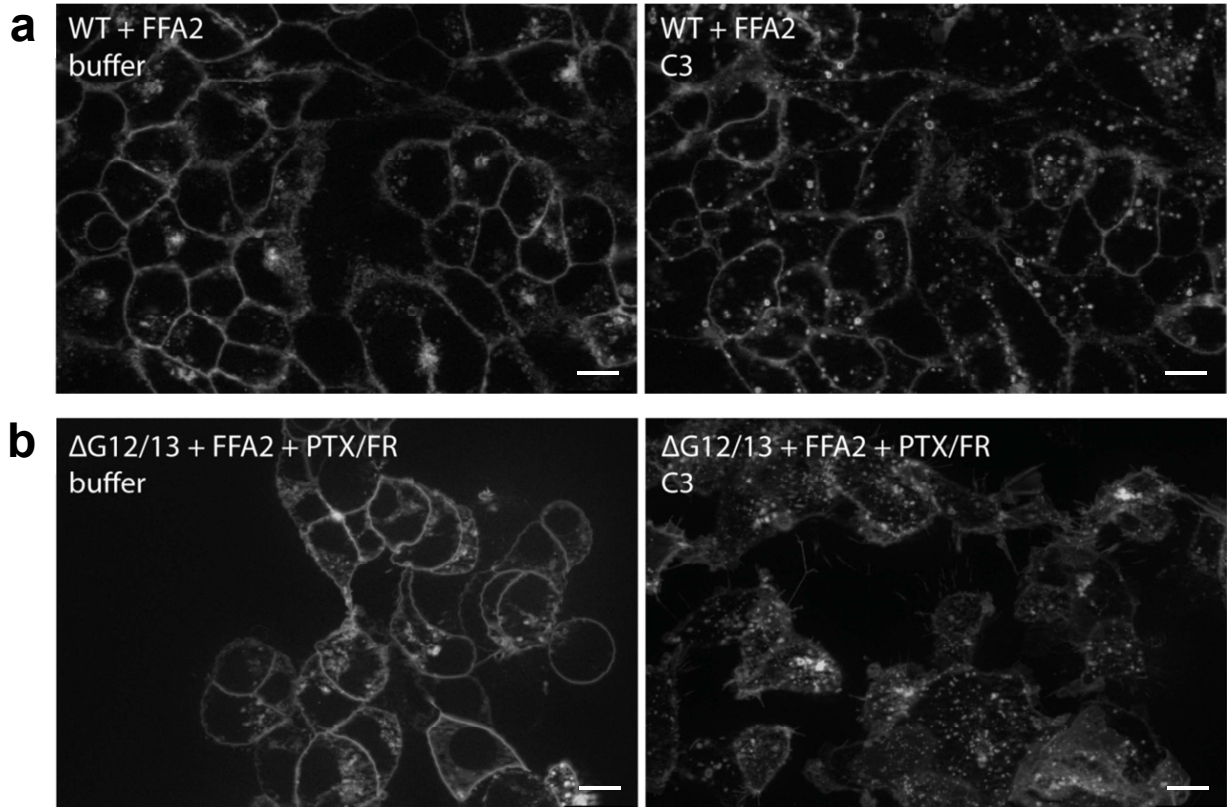
**Supplementary Figure 13. Biochemical characterization of  $\Delta\beta$ arr1/2 HEK293 cell lines using immunoblotting.** Western blots of lysates derived from wild-type (Parent) and three  $\Delta\beta$ arr1/2 HEK293 cell clones (#1, #2, #3) probed with antibodies against  $\beta$ -arrestin1 ( $\beta$ arr1) and  $\beta$ -arrestin2 ( $\beta$ arr2). Antibody against  $\beta$ -arrestin2 shows a minor non-specific band (asterisk). Western blot images are representative of two independent experiments with each showing similar patterns of immune-reactive bands. Unprocessed scans of Western blots are available in Supplementary Fig. 18.



**Supplementary Figure 14. DMR analysis of different HEK293 cell clones.** Quantification of DMR response towards multiple stimuli in wild-type (a), wild-type (parental) (b),  $\Delta\betaarr1/2$  clone #2 (c) and  $\Delta\betaarr1/2$  clone #3 (d). (e-h) AUC of DMR traces over the entire measurement time was analyzed and presented as mean values + SEM of 3 independent experiments, each measured in triplicates.

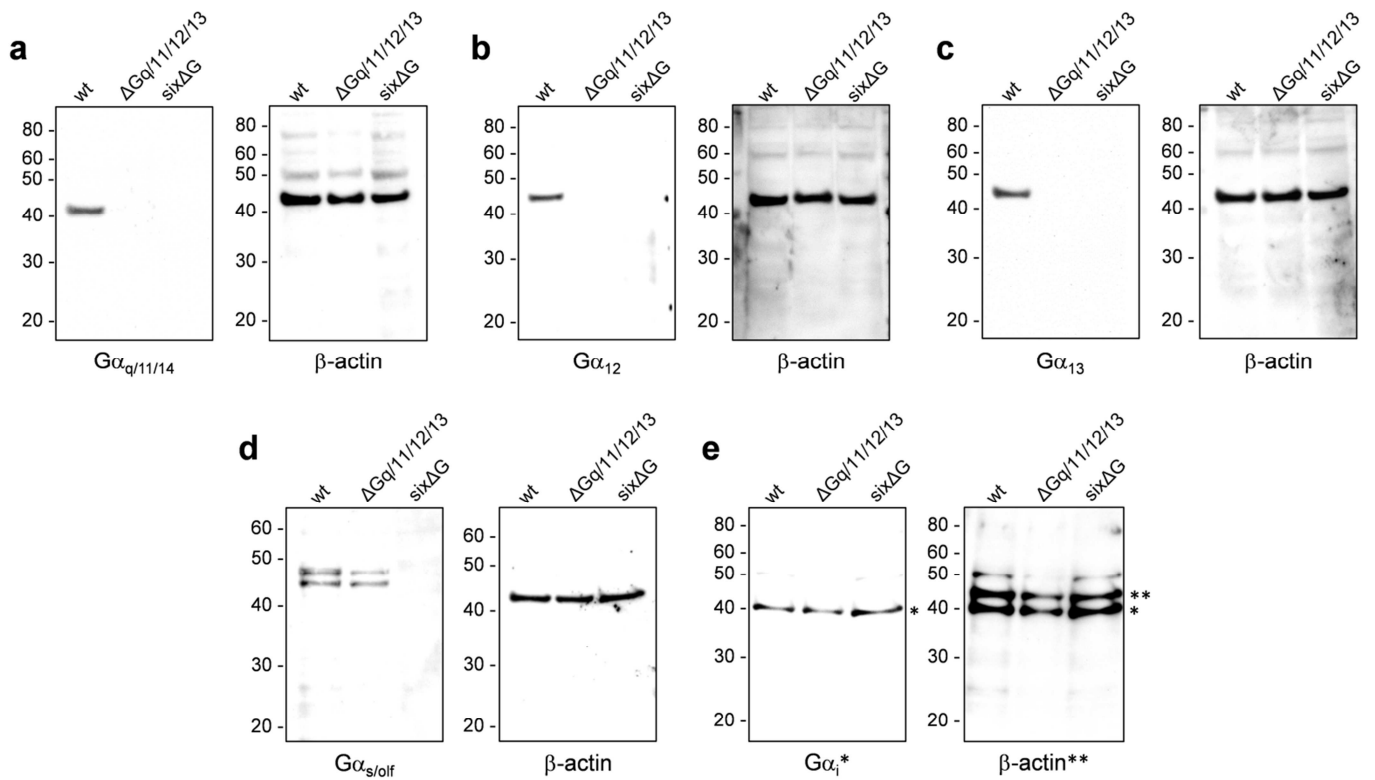


**Supplementary Figure 15. Agonist-mediated internalization in wild-type (parental) and  $\Delta\beta\text{arr}1/2$  HEK293 clones #1, #2, and #3.** Quantification of cell surface receptor abundance of FLAG-tagged Vasopressin V2 receptor (FLAG-V2R) (**a**) and FLAG-tagged  $\beta$ 2-adrenergic receptor (FLAG- $\beta$ 2AR) (**b**) in parental HEK293 cells (Parent) and  $\Delta\beta\text{arr}1/2$  clones #1, #2, and #3, either transfected with vector (Mock) or  $\beta$ -arrestin1 ( $\beta\text{arr}1$ ) or  $\beta$ -arrestin2 ( $\beta\text{arr}2$ ) and stimulated with 100 nM AVP (**a**) or 10  $\mu\text{M}$  Isoproterenol (Iso) (**b**). Data are mean + SEM of 4 independent experiments (3 technical replicates).

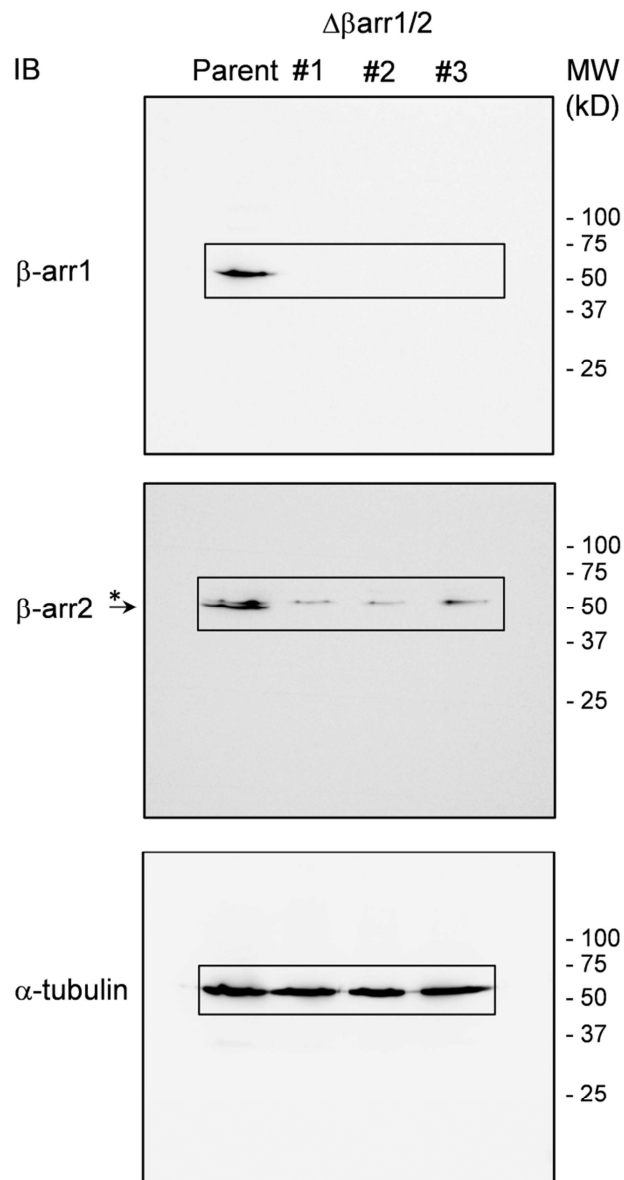


**Supplementary Figure 16. FFA2 receptor internalization in the absence of active G proteins.** Structured-illumination micrographs of YFP-tagged FFA2 receptors in wild-type (a) or  $\Delta G12/13$  (b) cells, imaged 30 minutes after buffer treatment (left panels) or stimulation with 100  $\mu M$  C3 (right panels). Scale represents 10  $\mu m$ ; representative images of 3 independent experiments.





**Supplementary Figure 17. Biochemical characterization of  $\Delta$ Gsix cells by immunoblot analysis. (a-e)** Uncropped images of Western blots shown in Supplementary Fig. 1a-e with wild-type,  $\Delta$ Gq/11/12/13 and  $\Delta$ Gsix HEK293 cell lysates probed against  $G\alpha_{q/11/14}$  (a),  $G\alpha_{12}$  (b),  $G\alpha_{13}$  (c),  $G\alpha_{s/olf}$  (d),  $G\alpha_i$  (e), and  $\beta$ -actin (a-e). (e) Note that  $G\alpha_i$  is also visible on the  $\beta$ -actin blot because  $G\alpha_i$  and  $\beta$ -actin antibody were from the same host species and corresponding immunoreactive bands were detected with similar illumination time (\*:  $G\alpha_i$ , \*\*:  $\beta$ -actin). Representative blots of 2 independent experiments.



**Supplementary Figure 18. Biochemical characterization of  $\Delta\beta\text{arr1/2}$  HEK293 cell lines using immunoblotting.** Unprocessed scans of Western blots presented in Supplementary Fig. 13 with lysates derived from wild-type (Parent) and three  $\Delta\beta\text{arr1/2}$  HEK293 cell clones (#1, #2, #3) probed against  $\beta$ -arrestin1 ( $\beta\text{arr1}$ ),  $\beta$ -arrestin2 ( $\beta\text{arr2}$ ) and  $\alpha$ -tubulin. Antibody against  $\beta$ -arrestin2 shows a minor non-specific band (asterisk). Cropped images are boxed. Blots are representative of 2 independent experiments.